# A Seamless Whole Speed Range Control of Interior PM Synchronous Machine without Position Transducer

Roman Filka*, Peter Balazovic*, Branislav Dobrucky†
* Freescale Semiconductor, 1. Maje 1009, Roznov p. Radhostem, Czech Republic
† University of Zilina/Department of Electrical Engineering, Univerzitná 1, 010 26 Žilina, Slovakia

*Abstract*— **This paper presents a complex solution for whole speed range sensorless control of interior permanent magnet synchronous motor (IPMSM) drives. To cover an entire speed range of IPMSM without position transducer, different sensorless techniques must be employed. Design and implementation of sensorless techniques for different operating speeds are described in this paper. Presented application has been implemented including the high frequency (hf) injection method and extended back EMF state observer on a single chip solution of DSC56F8300 series without any additional supportive circuitry.**

## I. Introduction

An important factor for using sensorless control in the drive applications is to optimize the total cost performance ratio of the overall drive cost. The systems should be less noisy, more efficient, smaller and lighter, more advanced in function and accurate in control with a low cost. To achieve efficient control of AC machines, knowledge of rotor position is essential. Different types of mechanical position transducers can be used to measure the rotor position directly. However solution with such transducer introduces additional cost, therefore alternative means of obtaining rotor position is highly desirable.

Sensorless control of AC machines has become a frequently discussed topic at engineering conferences. Many researchers and scientists have published papers on this topic but there are only a few articles that discuss complex implementation of the algorithms into a single application covering all operating conditions. One solution to sensorless control of the motor drive in applications such as air-condition units, fans, compressors is to use a brushless DC motor (BLDC). These motors have trapezoidal back-EMF, because of geometrical arrangement of the magnets in the rotor; therefore six step commutation control is sufficient [1]. Driving motor in six step commutation allows for observation of back-EMF zero crossing, since there is always an instant in switching sequence of the inverter, when both switches in one of the inverter leg do not conduct the current. Knowing the point of back-EMF zero crossing a subsequent commutation sequence can be calculated, thus allowing BLDC motor to operate without position transducer. Six step commutation control of BLDC however, has several drawbacks; such as low efficiency, higher audible noise and lower developed torque when compared to sinusoidal control of PMSM. To increase efficiency of the drive, sinusoidal control is needed [1]. Here, all three phases of the inverter are constantly conducting current making observation of back-EMF zero crossing impossible. Therefore more complex sensorless algorithms must be employed.

Sensorless algorithms for sinusoidal control of AC machines can be broadly divided into two major groups; 1.) Those that utilize magnetic saliency for tracking rotor position [2]-[12] and 2) those that estimate rotor position from calculating motor model [8],[13]-[16]. The later, requires accurate knowledge of phase voltages and current for proper functionality. At low speeds, phase voltage reference and measured phase current are low, making it very difficult to separate from noise. Also distortion by inverter non-linearities and model parameter deviation becomes significant with decreasing speed. Therefore methods based on motor model are not suitable for low rotor speeds. For start-up and low speeds, additional carrier signal superimposed to the main excitation is required. This carrier signal adds needed excitation to the motor at low and zero speed, and its back analysis can provide a viable means of obtaining information about rotor position. The carrier injection methods however, require a certain amount of saliency present in the motor [3]. In IPMSM this saliency results from inductance variation [1] as is explained later in the paper. On the other hand, at high speeds the amplitude of back EMF is big enough for motor model and angle tracking observer to work properly, therefore no additional signal is required. In fact, additional *hf* signal deteriorates tracking accuracy of the angle tracking observer. Therefore injection of *hf* signal is not desired for high speed operation. It is obvious, that in order to achieve full speed range sensorless operation of IPMSM, both techniques have to be employed, each covering different operational speed ranges. This requires algorithm that will ensure seamless blending of the estimates throughout the entire speed range.

The proposed solution is based on field oriented control of IPMSM with implemented speed control loop. This includes inner current control loop with implemented decoupling of cross-coupled variables achieving good torque control performance. To maximize converter efficiency and minimize its rating, current loop is designed with maximum torque/ampere criteria [1].

## II. IPMSM Characterization

### A. Motor Description

Mathematical model of IPM synchronous motor in synchronous reference frame is described as follows

$$\begin{bmatrix} u_d \\ u_q \end{bmatrix} = R_s \begin{bmatrix} i_d \\ i_q \end{bmatrix} + \begin{bmatrix} L_d s & L_q \omega_r \\ -L_d \omega_r & L_q s \end{bmatrix} \begin{bmatrix} i_d \\ i_q \end{bmatrix} + \psi_{PM} \omega_r \begin{bmatrix} 0 \\ 1 \end{bmatrix} \quad (1)$$

where

$s$ - differential operator;

$u_{dq}$ - stator voltages in synchronous reference frame;

$i_{dq}$ - stator currents in synchronous reference frame;

$L_{dq}$ - direct and quadrature inductances;

$\omega_r$ - rotor speed;

$\psi_{PM}$ - permanent magnet flux;

Torque developed by the IPM synchronous motors as described by (2), can be divided into two components. First component of the torque is created by contribution of the PM field $\psi_{PM}$ and is called synchronous torque. Second component, referred to as reluctance torque, arises due to rotor saliency, where the rotor tends to align with the minimum reluctance.

$$T_e = \frac{3}{2} p \left( \psi_{PM} i_q + \left( L_d - L_q \right) i_d i_q \right) \quad (2)$$

where

$p$ - number of pole pairs

IPM motors have the permanent magnets buried inside the rotor, which makes them salient pole machines with small effective air-gap. Reluctance in q-axis direction is smaller than that one in d-axis, resulting in q-axis inductance bigger than d-axis; $L_d < L_q$. Therefore in order to develop maximal torque according to (2), reluctance torque should be utilized i.e. $i_d$ current has to be adjusted to negative values, weakening the resulting magnetic field. On the other hand, the armature reaction effects are dominant, due to small effective air-gap, resulting in saturation of q-axis inductance according to level of applied load. This phenomenon is particularly important, because magnetic saliency decreases proportionally with saturated inductance and disappearing completely at certain load level. Furthermore under load the torque current in q-axis winding creates a term $\psi_{PM} i_q$ causing air-gap flux distribution to move towards direction of q-axis. Since the HF signal injection sensorless algorithm estimates the position of saliency rather than the position of rotor itself, this phenomenon has to be accounted for in the final application.

### B. *High Frequency Impedance*

In order to verify presence of magnetic saliency at high frequencies (*hf*), *hf* impedance measurements were carried out, as proposed by [4]. In these measurements, rotor is mechanically locked to prevent current signals distortion. *HF* signal of 50V/500Hz is injected in $d_m$ - axis of the measurement $d_m$-$q_m$ reference frame. This frame is shifted from actual rotor *d-q* frame by *angle_offset*. Offsetting the measurement frame will ensure correct alignment of the frames anytime the measurement is repeated. Since *angle_offset* is varied ±180 deg. electrical, at 90 deg. $i_{dm}$ will correspond to $i_{qm}$. Therefore to suppress DC offset of the $i_{dm}$ current under load, 1st order high pass filter with cut-off frequency 10Hz is used. Block diagram showing the *hf* impedance measurement algorithm as implemented on Digital Signal Controller is depicted on Fig. 1.

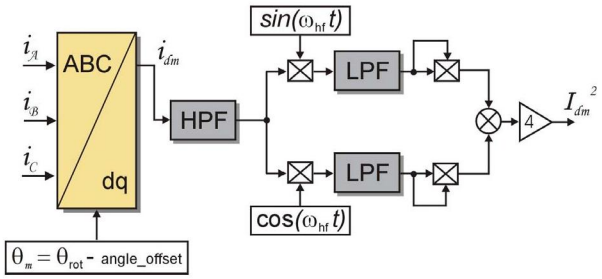


Fig. 1. Block diagram of HF impedance measurement.

Obtained measurement results are shown on Fig. 2, where resulting impedance is plotted as a function of *angle_offset* and load level. It can be seen from Fig. 2, that the saliency moves towards the direction of q-axis and disappears with increasing load level as assumed in section II. A. Saliency disappearing with increasing load will cause eventual failure of sensorless algorithm based on saliency tracking. This can be avoided by proper compensation action in d-axis current [4], which however will introduce additional losses in the motor and decrease the efficiency of the control loop.

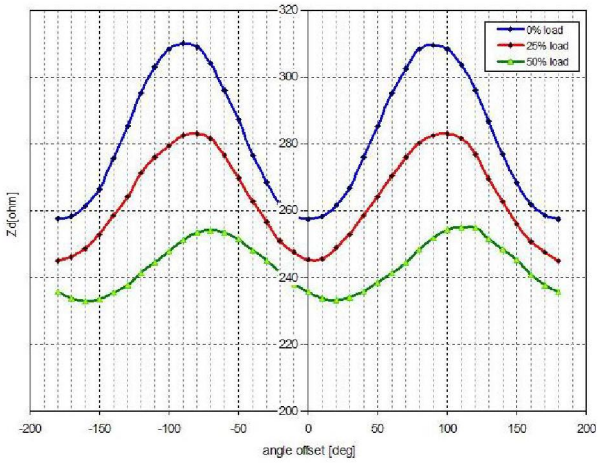


Fig. 2. High Frequency impedances as a function of difference between measurement and actual rotor reference frames and applied load.

## III. Design Of Sensorless Control For IPMSM

### A. *Initial Position Detection and Low Speed Sensorless Control*

As with any other synchronous motor, the first problem to overcome in FOC is the motor start-up. In contrast with AC induction motor where rotor flux is basically created from the stator, in IPM motor the rotor flux is created by permanent magnets present in the rotor. In order to be able to use FOC, position of this rotor flux has to be known prior to any control action. In conventional IPM control with an encoder as position transducer, initial position is set by applying DC voltage in one motor phase, which creates a magnetic pole attracting opposite pole of rotor magnets (alignment process). This process unavoidably generates often unwanted rotor movements. Sensorless

algorithm based on injection of pulsating hf signal in synchronous frame can be used to estimate the position of rotor at start-up. This sensorless approach is physically based on property of d and q axes flux being decoupled [3]. Therefore if an estimated $\hat{d}-\hat{q}$ reference frame is defined and not precisely aligned with a real rotor $d-q$ reference frame, then by applying flux vector at known carrier frequency for example in the $\hat{d}$ axis, current at carrier frequency can be observed in the $\hat{q}$ axis. This current is directly proportional to the misalignment angle of the estimated and rotor reference frame. Therefore changing the position of estimated frame such that this $\hat{q}$ axis current is zero or minimal, will allow for tracking of real rotor i.e. saliency position.

Considering high frequency signals, motor model from (1) can be rewritten into estimated reference frame (3). In this *hf* IPM synchronous motor model, voltage drop across the stator resistance and back-EMF components can be neglected.

$$\begin{bmatrix}\hat{u}_d\\ \hat{u}_q\end{bmatrix}=\begin{bmatrix}Z_1+\Delta Z\cos(2\theta_{err}) & -\Delta Z\sin(2\theta_{err})\\ -\Delta Z\sin(2\theta_{err}) & Z_1-\Delta Z\cos(2\theta_{err})\end{bmatrix}\begin{bmatrix}\hat{i}_d\\ \hat{i}_q\end{bmatrix} \quad (3)$$

where

$$Z_1=\frac{Z_d+Z_q}{2}\ ,\quad \Delta Z=\frac{Z_d-Z_q}{2}\ ,\quad \theta_{err}=\theta_{rot}-\theta_{est} \quad (4)$$

$\hat{u}_{dq}$ - stator voltages in estimated frame;

$\hat{i}_{dq}$ - stator currents in estimated frame;

$\theta_{rot}$ - rotor position;

$\theta_{est}$ - estimated position;

$\theta_{err}$ - position error;

Applying hf signal $u_{hf}=U_m\sin(\omega_{hf}t)$ in d-axis of *hf* model of (3), will result in hf currents

$$\begin{bmatrix}\hat{i}_d\\ \hat{i}_q\end{bmatrix}=-\frac{U_m}{\omega_{hf}Z_dZ_q}\cos\left(\omega_{hf}t\right)\begin{bmatrix}Z_1-\Delta Z\cos\left(2\theta_{err}\right)\\ \Delta Z\sin\left(2\theta_{err}\right)\end{bmatrix} \quad (5)$$

After filtering and demodulation, $\hat{i}_q$ current is described as

$$\hat{i}_q=-\frac{U_m\Delta Z}{2\omega_{hf}Z_dZ_q}\sin(2\theta_{err}) \quad (6)$$

The relationship between $\hat{i}_q$ and estimated position error from (6) suggest to use a controller capable of driving its output such that $\hat{i}_q$ current will remain zero. This can be a standard proportional-integrational (PI) controller.

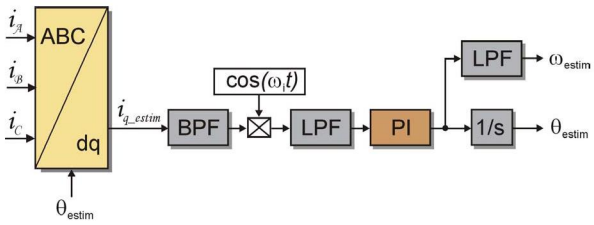


Fig. 3. Saliency tracking observer (STO); as used for rotor position estimation at zero and low speeds.

Output of the PI controller represents the estimated speed, thus its integration yields position of the estimated reference frame. Such structure acts as a phase locked loop and its schematic block diagram is depicted on Fig.3.

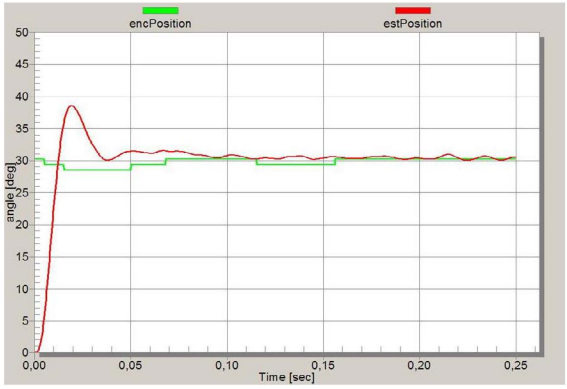


Fig. 4. Saliency tracking observer; initial position alignment.

Fig. 4 demonstrate experimental results of initial Saliency Tracking Observer (STO) alignment, which is used for start-up rotor position detection. The experiment is carried out with rotor manually rotated to arbitrary position and then running STO alignment process.

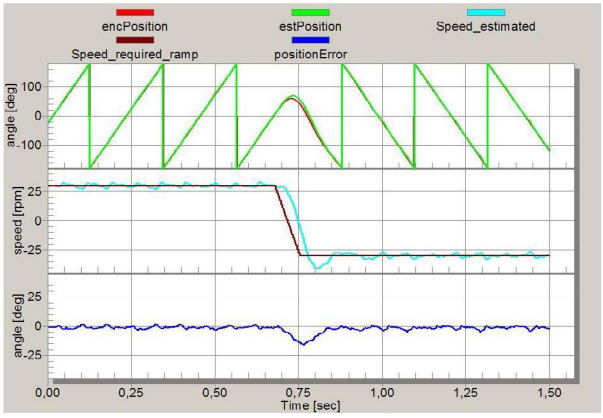


Fig. 5. Position error during reversal at 30rpm. IPMSM operated in full sensorless speed FOC.

Position error during speed reversal at 30 rpm is depicted on Fig. 5. Here the motor is operated in speed FOC with position and speed feedback provided by STO, i.e. full sensorless mode. Rotor position from encoder is used only for comparison with estimated position. Experimental results of low speed full sensorless control with speed reversal under different load conditions are shown on Fig. 6, and Fig. 7. Rotor position information from encoder is not used in these experiments.

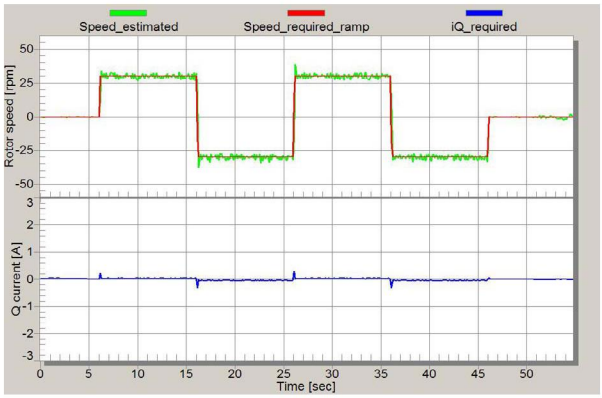


Fig. 6. Low speed full sensorless FOC, with speed reversal ±30 rpm under no load.

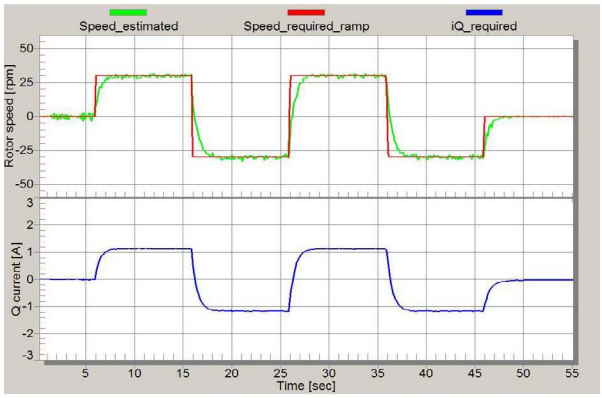


Fig. 7. Low speed full sensorless FOC, with speed reversal ±30 rpm under load (20% nominal).

## B. *High Speed Sensorless Control*

There have been proposed many sensorless control methods for surface permanent-magnet synchronous motors based on estimation of electromotive force in which the electrical position information of machine is encoded.

$$\underbrace{\begin{bmatrix} u_\alpha \\ u_\beta \end{bmatrix}}_{\vec{u_S}} = \underbrace{R_s \cdot \begin{bmatrix} i_\alpha \\ i_\beta \end{bmatrix}}_{\vec{u_R}} + \underbrace{pL_0 \cdot \begin{bmatrix} i_\alpha \\ i_\beta \end{bmatrix}}_{\vec{u_L}} + \underbrace{k_e \cdot \omega_e \cdot \begin{bmatrix} -\sin(\theta_e) \\ \cos(\theta_e) \end{bmatrix}}_{\vec{u_E}} + \underbrace{2 \cdot \omega_e \cdot \Delta L \cdot \begin{bmatrix} -\sin(2\theta_e) & \cos(2\theta_e) \\ \cos(2\theta_e) & \sin(2\theta_e) \end{bmatrix} \cdot \begin{bmatrix} i_\alpha \\ i_\beta \end{bmatrix}}_{\vec{u_{REL}}} \tag{7}$$

Fundamentally, these estimation methods for the position and velocity are based on the motor mathematical model. However, mentioned methods cannot be directly applied to an interior permanent-magnet synchronous motor, because the position information is contained not only in the conventionally defined back electro-motive force (EMF) but also in the definition of stator inductance as shown in (7).

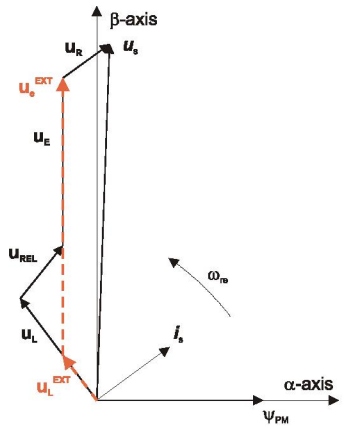


Fig. 8. Vector diagram of salient-pole machine.

The vector representation of given equation (7) is displayed in Fig. 8. Unfortunately, the computation of position dependent information which is contained in two unknown voltage vectors conventional $\mathbf{u_E}$, and $\mathbf{u_{REL}}$ makes difficulties to assess it. However, there has been proposed [13] a simple way to resolve this problem by eliminating the $2\theta_e$ term in (7) using purely mathematical method. Here is described a mathematical model of interior PMSM motor which is based on an extended electro-motive force function [13]. This extended electro-motive force (EEMF) model includes both position information from the conventionally defined EMF and the stator inductance as well. Then, it makes possible to obtain the rotor position and velocity information by estimating the extended EMF only.

$$\underbrace{\begin{bmatrix} u_\alpha \\ u_\beta \end{bmatrix}}_{\vec{u_S}} = \underbrace{R \cdot \begin{bmatrix} i_\alpha \\ i_\beta \end{bmatrix}}_{\vec{u_R}} + \underbrace{\begin{bmatrix} pL_d & (L_d - L_q)\cdot\omega_e \\ -(L_d - L_q)\cdot\omega_e & pL_d \end{bmatrix} \cdot \begin{bmatrix} i_\alpha \\ i_\beta \end{bmatrix}}_{\vec{u_L^{EXT}}} + \underbrace{\left\{(L_d - L_q)(\omega_e i_d - i'_q) + k_e \cdot \omega_e\right\} \cdot \begin{bmatrix} -\sin(\theta_e) \\ \cos(\theta_e) \end{bmatrix}}_{\vec{u_E^{EXT}}} \tag{8}$$

In this equation (8) there is no $2\theta_e$ dependent term comparing to conventionally defined IPMSM machine model (7). The second term $\mathbf{u_L}^{\mathbf{EXT}}$ and third term $\mathbf{u_E}^{\mathbf{EXT}}$ on the right side of equation (8) are depicted in Fig. 11 as vectors in dashed yellow lines. The $\mathbf{u_L}^{\mathbf{EXT}}$ vector term in equation (8) can be explained as extension of conventional inductance voltage drop, and second vector term $\mathbf{u_E}^{\mathbf{EXT}}$ is considered as an extension of conventional back EMF term. It is obvious that extended inductance voltage drop $\mathbf{u_L}^{\mathbf{EXT}}$ has no position dependent information and only extended back EMF term $\mathbf{u_E}^{\mathbf{EXT}}$ possesses position dependent information. This rewritten mathematical model of interior PMSM motor makes possible to express the extended back EMF term $\mathbf{u_E}^{\mathbf{EXT}}$ to be simply estimated using standard estimation approach of surface-mounted PMSM motor.

$$\begin{bmatrix} u_{e\alpha} \\ u_{e\beta} \end{bmatrix} = \left\{(L_d - L_q)(\omega_e i_d - i'_q) + k_e \cdot \omega_e\right\} \cdot \begin{bmatrix} -\sin(\theta_e) \\ \cos(\theta_e) \end{bmatrix} \tag{9}$$

In eq. (9), besides the conventionally defined EMF generated by the permanent magnet, there is a kind of voltage related to the saliency of the interior PMSM

motor. It includes the position information from both the EMF and the stator inductance. It is a general form of mathematical model for all the synchronous motors [13].

### C. State Observer of Extended Back EMF

In this section described state observer is applied to interior PMSM motor with an estimator model excluding the extended EMF term. Then extended EMF term can be estimated using the state observer as depicted in Fig. 9, which utilizes a simple observer of IPM motor stator current. Here presented state observer is realized within stationary reference frame ($\alpha\beta$). The estimator of α-axis consists of the stator current observer based on $RL$ motor circuit with estimated motor parameters. This current observer is fed by the sum of the actual applied motor voltage ($u_\alpha$), cross-coupled rotational term which corresponds to the motor saliency $\Delta L$ and compensator $F_{c\alpha}(s)$ corrective output. Since extended term of back EMF is not included in the interior PMSM motor observer model, the compensator $F_{c\alpha}(s)$ corrective output shown in Fig. 9 supplies the not modeled extended back EMF [14],[15]. The estimate of extended EMF term in α-axis can be derived as follows

$$\hat{E}_\alpha(s) = F_c(s)\cdot\left[I_\alpha(s) - \hat{I}_\alpha(s)\right] \qquad (10)$$

It is obvious that the accuracy of the back EMF estimates is determined by the correctness of used motor parameters (R, L) by fidelity of the reference stator voltage and by quality of compensator such as bandwidth, phase lag and so on. It is obvious from the extended EMF transfer function that even if motor parameters are precisely matched, the estimates are limited by compensator quality. This implies that state observer bandwidth and its corresponding phase lag constraints the performance of used method. The same consequences apply for estimate of the extended EMF in β-axis.

The angle tracking observer [16] shown in Fig. 9 is widely used for the estimation of the rotor angle. By employing the tracking observer, noise on the position estimate can be filtered out without adding lag to the estimate within its bandwidth [14],[16]. The primary benefit of the angle tracking observer utilization, in comparison with the trigonometric method, is its smoothing capability [17].

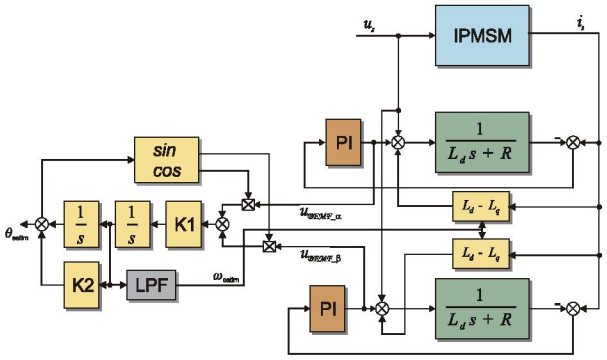


Fig. 9. Block diagram of state observer of extended back EMF.

### D. Experimetal Results of Extended Back EMF State Observer

The extended back EMF state observer has been implemented using digital signal controller of Freescale's 56F8300 series with interior PMSM. The motor with parameters summarized in Table I has been used for these experiments.

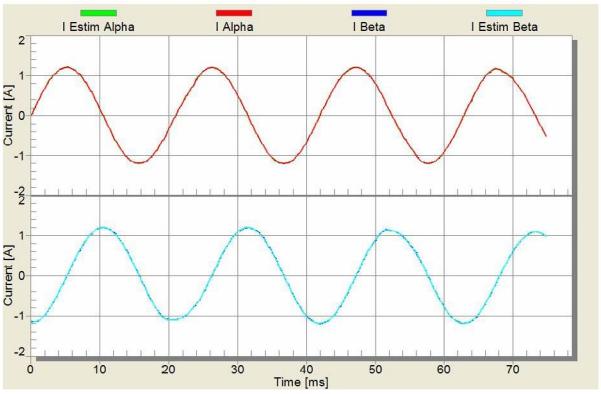


Fig. 10. Estimated $\alpha\beta$ currents by state observer at 300 [rad.sec$^{-1}$].

Electrical rotor position and speed are fed back from encoder transducer, and are granted as reference to estimated values of rotor electrical position $\theta_{estim}$ and angular speed $\omega_{estim}$. This motor drive operation allows evaluating the quality of sensorless algorithm. The observer tracking capability of phase stator currents expressed in stationary reference frame are evaluated as shown in Fig. 10.

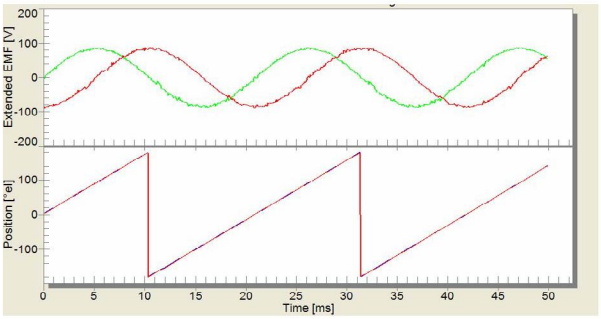


Fig. 11. Estimated extended EMF by state observer at 300[rad.sec$^{-1}$] and estimated electrical position by angle tracking observer.

The IPM synchronous motor under test have been operated in tracking mode, where speed control has attained the position and speed from encoder, and estimation algorithm tracks actual rotor position. As can be seen from Fig. 10, the estimation of speed and position have very good accuracy and apparently the encoder position feedback can be replaced by these estimates from the extended back EMF state filter. The controller output, which corrects motor phase currents, is supplying part of the motor state which is not modelled, i.e. the extended back EMF. Fig. 11 shows the estimated extended back EMF at 300 [rad.sec$^{-1}$].

If the IPM synchronous motor drive operates in sensorless mode, the electrical position required for vector transformation is attained from sensorless algorithm and feedback speed control loop is formed by state observer estimate. Satisfactory sensorless operation was also

achieved under different operation condition. As can be seen from Fig. 11 there is a very high correspondence between estimated rotor position (red) and encoder measurement of electrical position (blue). The exact knowledge of rotor position is very critical to IPM motor stable operation and it is seen that in sensorless mode the IPM motor functions with minimum sensitivity to motor load having very high agreement of measured position from encoder and state filter estimate.

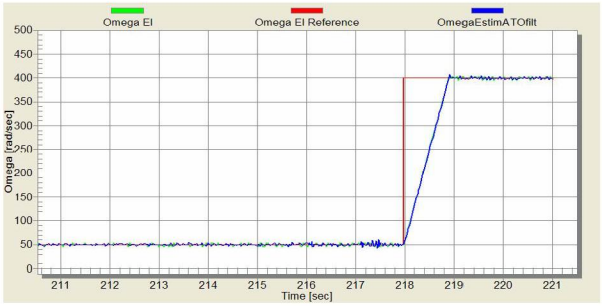


Fig. 12. Speed control with ramp acceleration under load condition.

Since state observer sensorless algorithm operates reliable from 50 [rad.sec$^{-1}$], the speed command is demanded from this limit. Speed acceleration from 50[rad.sec$^{-1}$] up to 400[rad.sec$^{-1}$] is shown on Fig. 12. As is apparent, almost identical behaviour of estimated and encoder speed was achieved. The operation of sensorless IPM motor drive has also been tested under variable load condition as shown in Fig. 13. Here the motor was in steady state and step change in motor load was applied.

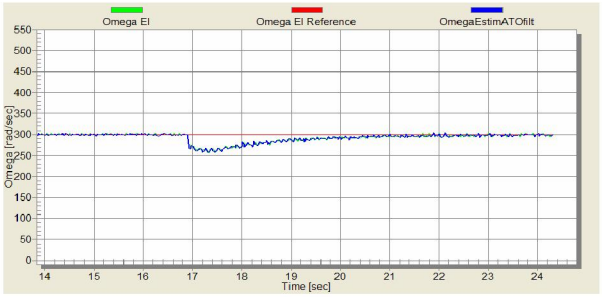


Fig. 13. Sensorless speed control at step change in load.

## E. *Whole Speed Sensorless Control*

In order to fully control IPM synchronous motor throughout the entire speed range, estimates from low and high speed sensorless algorithms have to be evaluated and merged. Proposed merging algorithm is based on cross-over functions, assuring smooth transition between algorithms. Moreover using cross-over functions allows completely switching off the algorithm currently not used [8], thus minimizing losses due to *hf* injection at high speeds. Fig. 13 shows block diagram of algorithms for whole speed sensorless control of IPM synchronous motor.

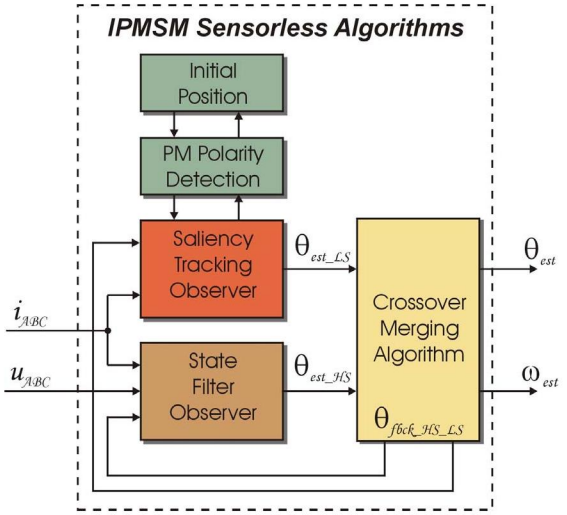


Fig. 13. Block diagram of IPMSM sensorless algorithms for entire speed range.

Block diagram of IPM synchronous motor field oriented control with sensorless position/speed feedback is depicted on Fig. 14. Fig 15 shows experimental results of full IPM synchronous motor sensorless control obtained from experimental setup according to Fig. 14. In this experiment the motor is operated in speed FOC with estimated position/speed provided by merging algorithm.

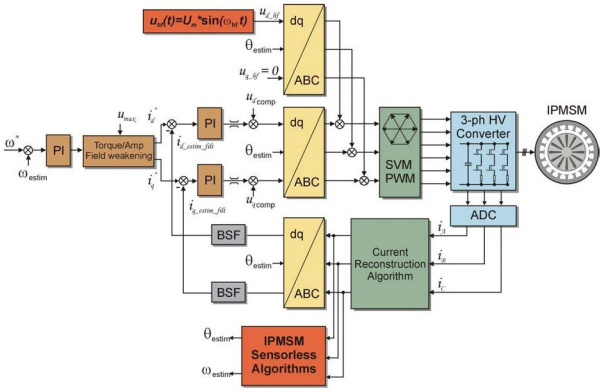


Fig. 14. Overall structure of IPMSM sensorless field oriented control with speed loop.

Position error is calculated with respect to position obtained from encoder. Encoder is used only for comparisons.

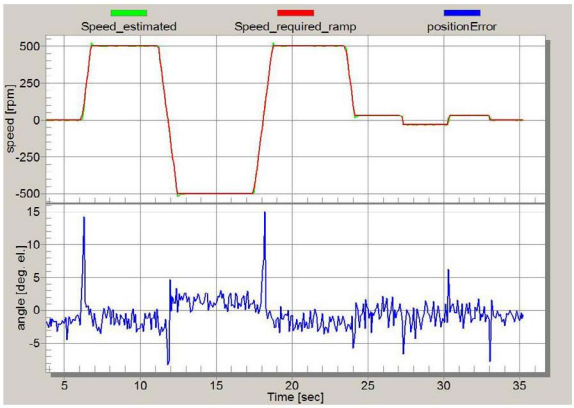


Fig. 15. Whole speed range full sensorless control with speed reversal. IPMSM operated in speed sensorless FOC.

TABLE I.
MOTOR PARAMETERS

| MOTOR PARAMETER | VALUE |
|---|---|
| Number of poles | 20 |
| Rated speed | 600 [rpm] |
| Phase voltage max. | AC 200 [V] |
| Phase current max | 8A p-p |
| Ke | 0.255 [V.sec/rad] |
| Rs | 7.5 [Ω] |
| Ld | 0.081 [H] |
| Lq | 0.095 [H] |

## IV. CONCLUSION

Sensorless field oriented control of IPMSM covering the entire speed range has been presented. Merging algorithm based on cross-over function has been designed in order to perform a smooth transition between two different sensorless algorithms. Presented approach by this paper is based on *hf* signal injection method for low speed operation and on the estimation of an extended EMF in the stationary reference frame using a state filter for high speed operation. The spatial information obtained from the estimates of extended EMF is used in an angle tracking observer to estimate the rotor electrical position. The extended EMF model includes both position information from the conventionally defined EMF and the stator inductance. This makes it possible to obtain the rotor position and velocity information by estimating the extended EMF only. Whole implementation of transient injection method and extended back EMF state filter has been achieved on a single chip solution of DSC56F8300 series without any additional supportive circuitry.

## REFERENCES


[1] B. Bose, *Modern Power Electronics and AC Drives*, Prentice Hall PTR, 2002.

[2] P. Vadstrup, R. D. Lorenz, "Robust Estimator Design for Signal Injection-Based IPM Synchronous Machine Drives" in. *Trans. of IEEE-IAS,* 2004, pp 957-963.

[3] J. Ha, S. K. Sul, K. Ide, I Murokita, K. Sawamura, "Physical Understanding of High Frequency Injection Method to Sensorless Drives of an Induction Machine" in. *Trans. of IEEE,* 2000, pp 1802-1808.

[4] J. Ha, K. Ide, T. Sawa, and S. K. Sul, "Sensorless Position Control and Initial Position Estimation of an Interior Permanent Magnet Motor" in. *Trans. of IEEE-IAS,* 2001, pp 2607-2613.

[5] Y. Jeong, R. D. Lorenz, T. M. Jahns, S. K. Sul, "Initial Rotor Position Estimation of an Interior Permanent-Magnet Synchronous Machine Using Carrier-Frequency Injection Methods" in. *IEEE Trans. on IA,* vol. 41, No. 1, Jan./Feb. 2005, pp 38-45.

[6] H. Kim, K. K. Huh, R. D. Lorenz, and T. M. Jahns, "A Novel Method for Initial Rotor Position Estimation for IPM Synchronous Machine Drives" in. *Proceedings of IEEE,* 2003, pp 1173-1180.

[7] S. Ogasawara, H. Akagi, „An Approach to Real-Time Position Estimation at Zero and Low Speed for a PM Motor Based on Saliency", in *IEEE Trans. on Industry Applications*, No. 1, Jan./Feb. 1998, pp. 163-168.

[8] H. Kim, S. Yi, N. Kim, and R. D. Lorenz, "Using Low Resolution Sensors in Bumpless Position/Speed Estimation Methods for Low Cost PMSM Drives" in. *Trans. of IEEE-IAS,* 2005, pp 2518-2525.

[9] J. M. Kim, S. K. Sul, "Speed Control of Interior Permanent Magnet Synchronous Motor Drive for the Flux Weakening Operation" in. *Trans. of IEEE,* vol. 33, No. 1, Jan./Feb. 1997, pp 43-48.

[10] K. Ide, J. Ha, M. Sawamura, H. Iura, and Y. Yamamoto "High Frequency Injection Method Improved by Flux Observer for Sensorless Control of an Induction Motor" in. *Proceedings of PCC-Osaka,* 2002, pp 516-521.

[11] B. Dobrucký, P. Balažovič, R. Filka, Abdalmula M.A.R., „Robotic Servo-System with Sensorless Measurement of Initial Position of PMSM Motor Using PC&ADSP21062 Control", in *Proceedings of RAAD'01 conference,* Vienna (AT), May 2001.

[12] Abdalmula M.A.R., B. Dobrucký, P Pavelka, „Combined Method for Position Determination of PMSM in Zero- and Low Range of the Speed", in *Proc. of EDPE'03 conf.*, Sep. 2003

[13] Z. Chen, M. Tomita, S. Doki, S. Okuma, "An extended electromotive force model for sensorless control of interior permanent-magnet synchronous motors", in *IEEE Trans. on Industrial Electronics*, vol. 50, no. 4, April 2003, pp. 288-295.

[14] H. Kim, M.C. Harke, R.D. Lorenz, "Sensorless control of interior permanent-magnet machine drives with zero-phase lag position estimation", in *IEEE Trans. on Industry Applications*, vol. 39, no. 1, Jan.-Feb. 2003, pp. 1726-1733.

[15] R.D. Lorenz, "Observers and state filters in drives and power electronics", in *Conf. Rec. of the IEEE IAS OPTIM*, May 2002.

[16] M. Mienkina, P. Pekarek, F. Dobes, "56F80x resolver driver and hardware interface", in *Application Note AN1942*, Freescale Semiconductor Inc., 2005.

[17] R. Filka, P. Balazovic, "Intelligent sensorless control of AC permanent magnet motors," in *Embedded Control Europe*, October 2005, pp. 17-19.